Survival analysis of histopathological image based on a pretrained hypergraph model of spatial transcriptomics data

Shangyan Cai[1,2], Weitian Huang[2,3], Weiting Yi[3], Bin Zhang[2], Yi Liao[3], Qiu Wang[2], Hongmin Cai[3], Luonan Chen[2,⋆], Weifeng Su[1⋆]

[1] Division of Science and Technology, Beijing Normal University-Hong Kong Baptist University United International College, Zhuhai 519087, China
[2] Guangdong Institute of Intelligence Science and Technology, Hengqin, Zhuhai 519031, China
[3] School of Computer Science and Engineering, South China University of Technology, Guangzhou, 510006, China

Abstract. Survival analysis is critical for clinical decision-making and prognosis in breast cancer treatment. Recent multimodal approaches leverage histopathology images and bulk RNA-seq to improve survival prediction performance, but these approaches fail to explore spatial distribution at the cellular level. In this work, we present a multimodal hypergraph neural network for survival analysis (MHNN-surv) that introduces a pre-trained model for spatial transcriptomic prediction. The method is characterized by making full use of histopathological images to reveal both morphological and genetic information, thus improving the interpretation of heterogeneity. Specifically, MHNN-surv first slices Whole-Slide Imaging (WSI) into patch images, followed by extracting image features and predicting spatial transcriptomic, respectively. Subsequently, an image-based hypergraph is constructed based on three-dimensional nearest-neighbor relationships, while a gene-based hypergraph is formed based on gene expression similarity. By fusing the dual hypergraphs, MHNN-surv performs an in-depth survival analysis on breast cancer using the Cox proportional hazards model. The experimental results demonstrate that MHNN-surv outperforms the state-of-the-art multimodal models in survival analysis.

Keywords: Survival analysis · Multimodal data integration · Hypergraph neural networks.

1 Introduction

Survival analysis is a pivotal statistical tool in medical research [1], where it quantitatively evaluates the time until an event of interest, such as recurrence or mortality. Survival risk stratification is crucial for understanding the variability

⋆ Weifeng Su, Luonan Chen are the Co-corresponding Authors, E-mail: wfsu@uic.edu.cn, lnchen@sibcb.ac.cn.

in breast cancer progression and outcomes, thereby aiding clinicians in personalizing treatment strategies [2]. The adoption of Whole Slide Imaging (WSI) has significantly advanced survival analysis by providing detailed histopathological insights that surpass the capabilities of traditional manual microscopy, enhancing the accuracy of prognostic models [3]. However, the reliance on WSI alone, a single-modality approach, is limited by focusing solely on morphological features. This limitation fails to account for the genetic and molecular dynamics that significantly influence tumor behavior and patient prognosis, highlighting the necessity for the integration of gene expression data into survival analysis [4,5]. Consequently, integrating gene expression and WSI could enrich the survival analysis, offering a comprehensive view of the tumor's biology and substantially enhancing the prognostic performance of models [6,7].

Nonetheless, current multimodal approaches that utilize bulk RNA sequencing encounter a critical limitation of the absence of spatial resolution, which aggregates data from thousands of cells, obscuring the detailed intratumoral heterogeneity. The precise spatial distribution of gene expression is crucial for a thorough understanding of the tumor microenvironment [8], thus facilitating treatment response prediction and tumor progression pathway elucidation [9]. In detail, areas within tumors with high expression levels of genes associated with aggressive cancer growth may indicate poor prognosis [10]. Additionally, the spatial data may identify microenvironmental niches within tumors resulting in resistance to standard therapies, thereby facilitating the design of targeted therapies [11]. Consequently, introducing the spatial information into survival analysis cooperating with gene expression and WSI could leverage comprehensive information to achieve more accurate prognostic predictions, which will fill the crucial gap in the design of multimodal prognostic models.

Herein, we aim to utilize spatial transcriptomic data for survival analysis, countering the lack of spatially informed gene expression due to the limited availability and high cost of spatial transcriptomic technology. This paper introduces a novel model, the Multimodal Hypergraph Neural Network (MHNN-surv), which leverages Whole Slide Image (WSI) data to predict gene expressions with spatial details, aiming to address the data acquisition challenges and enhance the multimodal prognostic model with comprehensive spatial insights, as illustrated in Fig.1. MHNN-surv begins by standardizing WSI data through an intensive preprocessing stage for dependable feature extraction. Subsequently, it constructs dual hypergraphs: one based on image data and another on gene expressions, reflecting the tissue's morphological complexities and spatial gene expression. Finally, MHNN-surv integrates these hypergraphs to learn a global representation of WSI, enabling enhanced survival analysis with precise prognostic predictions.

The proposed model is a comprehensive multimodal learning framework that integrates diverse modalities with global structure consistency. The contributions of this work are summarized as follows:

- To the best of our knowledge, this is the first work to introduce spatial transcriptomic data for survival analysis, with mitigating the absence of paired spatial genomics data and survival information cohorts.
- We propose a novel model named MHNN-surv to leverage a dual hypergraph neural network to integrate the comprehensive information of WSI data, gene expression, and spatial information for survival analysis, thus enhancing cancer prognostics performance with spatial gene expression insights.
- The integration of dual hypergraphs on multimodal data performs a comprehensive and in-depth survival analysis on breast cancer, with the experimental results demonstrating the superior performance of MHNN-surv in comparison of the state-of-the-art multimodal models.

2 Related Work

2.1 Multimodal Deep Learning for Survival Analysis

Multimodal approaches have aimed to combine Whole Slide Imaging (WSI) with genomic data, especially gene expression profiles. This strategy seeks to amalgamate the morphological insights from WSI with the genetic drivers of cancer progression, thereby portraying a fuller biological narrative. Proposals such as Multimodal Autoencoders aim to predict different subtypes of breast cancer patients and their survival [14]. An unsupervised method is developed to encode multimodal patient data into a universal feature representation independent of data type or modality [15]. Moreover, MGCN-CalRF utilizes a multimodal graphical convolutional network with calibrated classifier models from random forests for accurate prognosis prediction of human breast cancer [16]. Such multimodal models have proven that integrative models markedly enhance survival predictions over histology-only approaches.

2.2 Hypergraph Applications in Biomedical Computing Research

Hypergraphs excel in modeling complex and higher-order relationships between entities, making them ideal for managing the intricate nature of cancer data. Unlike Graph Neural Networks (GNN), HyperGraph Neural Networks (HGNN) capture both pairwise and group interactions, suitable for addressing cancer's layered complexity [13]. In survival analysis, HGNN effectively integrates diverse data sources and embraces the collective dynamics of biological systems. Several studies highlight their ability to identify critical gene sets and perform enrichment analysis, showcasing the versatility of hypergraphs in biological data analysis [12]. The multifactorial nature of cancer justifies integrating morphological and genetic influences on patient outcomes using hypergraphs. Our framework not only offers a more accurate depiction of the tumor environment but also improves prognostic efficacy, positioning it as a progressive solution in survival analysis.

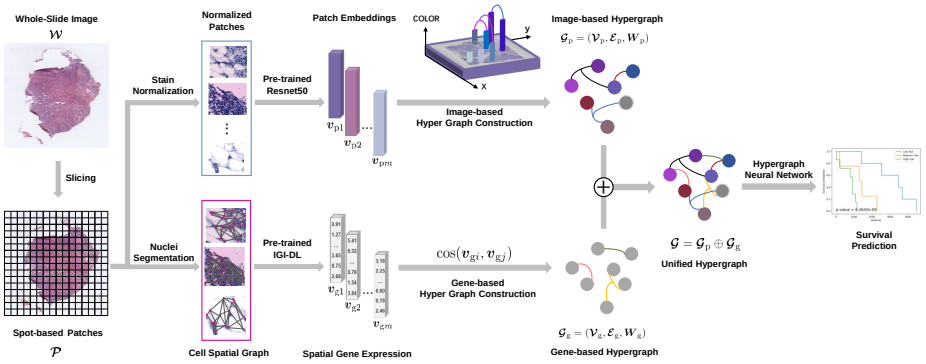

Fig. 1: MHNN-surv: An integrated framework for survival prediction using multimodal hypergraph neural networks. Spot-based patches are sliced from WSI and utilized to construct dual hypergraphs. By fusing two hypergraphs, it learns a global WSI representation to predict clinical outcomes.

3 Proposed Method

3.1 Problem Formulation

Given a WSI dataset of n samples, $\boldsymbol{\mathcal{W}}$, each histopathological image is sliced to a set of patches $\boldsymbol{\mathcal{P}} = \{\boldsymbol{P}_1, \boldsymbol{P}_2, \ldots, \boldsymbol{P}_m\}$. The size of the patch is set to 224×224, which is consistent with the spot of the spatial transcriptomic. Since the extracted patches may contain background areas that do not contain enough cells for further study, we retain patches with a tissue density greater than 0.7. These patches are used to extract image features and build image-based hypergraphs $\boldsymbol{\mathcal{G}}_{\mathrm{p}}$, as well as to predict gene expression and construct gene-based hypergraphs $\boldsymbol{\mathcal{G}}_{\mathrm{g}}$. Ultimately, a unified hypergraph $\boldsymbol{\mathcal{G}}$ is fused for predicting clinical outcomes by applying Cox proportional hazard model [18] to calculate the hazard rate as,

$$h(t|\boldsymbol{\mathcal{P}}) = h_0(t) \exp(f_{\boldsymbol{\theta}}(\boldsymbol{\mathcal{P}})). \tag{1}$$

where $h(t|\boldsymbol{\mathcal{P}})$ is the hazard function at time t for an individual with a given patch images $\boldsymbol{\mathcal{P}}$, $h_0(t)$ corresponds to the baseline hazard, and $f_{\boldsymbol{\theta}}(\boldsymbol{\mathcal{P}})$ represents the risk score derived from the MHNN-surv model with the parameters $\boldsymbol{\theta}$.

3.2 Dual Hypergraphs Construction

Image-based hypergraph construction. Due to the color of histology samples stained with H&E often varying between and within laboratories and from one batch to the next, we standardize the staining variance and brightness of selected patches with the help of StainTools [4].

[4] `https://github.com/Peter554/StainTools`

For constructing the image-based hypergraph $\boldsymbol{\mathcal{G}}_{\mathrm{p}} = (\boldsymbol{\mathcal{V}}_{\mathrm{p}}, \boldsymbol{\mathcal{E}}_{\mathrm{p}}, \boldsymbol{W}_{\mathrm{p}})$, the 2048-dimensional features of patches are extracted RestNet50 pre-trained on ImageNet and set as the vertex set $\boldsymbol{\mathcal{V}}_{\mathrm{p}} = \{\boldsymbol{v}_{\mathrm{p}1}, \boldsymbol{v}_{\mathrm{p}2}, \ldots, \boldsymbol{v}_{\mathrm{p}m}\}$, $\boldsymbol{v}_{\mathrm{p}i} \in \mathbb{R}^{2048}$. Conventionally, we set $\boldsymbol{W}_{\mathrm{p}} = \mathrm{I} \in \mathbb{R}^{k\times k}$, k denotes the number of image-based hyperedges. As for the hyperedge set $\boldsymbol{\mathcal{E}}_{\mathrm{p}} = \{\boldsymbol{e}_{\mathrm{p}1}, \boldsymbol{e}_{\mathrm{p}2}, \ldots, \boldsymbol{e}_{\mathrm{p}k}\}$, in contrast to the traditional computation of the two-dimensional Euclidean distance metric, we use pixel values indicating color as a third dimension to measure pairwise distances in 3-dimensional space. The inspiration comes from the fact that although some patches are physically close to each other in tissue, histopathological images may reveal that they belong to different tissue layers. The third dimension of i-th node $\boldsymbol{v}_{\mathrm{p}i}$ is computed by weighted color feature z_i to augment the morphological analysis with histopathological image color insights,

$$z_i = \frac{r_i \cdot V_r + g_i \cdot V_g + b_i \cdot V_b}{V_r + V_g + V_b}, \tag{2}$$

where r_i, g_i, and b_i denote the average value of the RGB channels in the i-th patch, V_r, V_g, and V_b are calculated by the variance of the RGB values of the neighboring 10 patches. In this way, a hypergraph $\boldsymbol{e}_{\mathrm{p}i}$ can be collected by computing the 3D Euclidean distances of pairs of patches and then connecting K nearest neighbor nodes,

$$d(\boldsymbol{v}_{\mathrm{p}i}, \boldsymbol{v}_{\mathrm{p}j}) = \sqrt{(x_i - x_j)^2 + (y_i - y_j)^2 + (z_i - z_j)^2}. \tag{3}$$

Gene-based hypergraph construction. After extracting patches from whole slide images (WSI), we built a Nuclei-Graph using the HoVer-Net model for nuclei segmentation and classification. Features including morphometric data and texture descriptors are extracted for each nucleus. The edges of the graph are determined based on spatial proximity. Meanwhile, we utilized an IGI-DL model [24] pre-trained on spatial transcriptomic data to predict the 69-dimensional gene expression profile of breast cancer at the spot level.

The gene-based hypergraph $G_g = (V_g, E_g, W_g)$ is desired to utilize spatial transcriptome of the patches as the vertex set and build hyperedges based on the similarity of gene expression, where $V_g = \{v_{g1}, v_{g2}, \ldots, v_{gm}\}, v_{gi} \in \mathbb{R}^{69}$, comprises 69-dimensional gene expression profiles. Here, we set $W_g = I^{l\times l}$, l denotes the number of gene-based hyperedges. For constructing the hyperedge set $E_g = \{e_{g1}, e_{g2}, \ldots, e_{gk}\}$, the cosine similarity is calculated to measure the pairwise similarity and collect K nearest neighbor nodes into a hypergraph:

$$\cos(v_{gi}, v_{gj}) = \frac{v_{gi} \cdot v_{gj}}{\|v_{gi}\|\|v_{gj}\|} \tag{4}$$

3.3 Hypergraph Fusion for Survival Analysis

MHNN-surv incorporates an innovative fusion strategy that synergizes dual hypergraphs, integrating morphological features from Whole Slide Images (WSI) and spatially predicted gene expression data into a cohesive framework.

Fusion strategy. The goal is to merge the vertices and edges ofdual hypergraphs into a unified hypergraph $\boldsymbol{\mathcal{G}} = (\boldsymbol{\mathcal{V}}, \boldsymbol{\mathcal{E}}, \boldsymbol{W})$,

$$\begin{aligned} \boldsymbol{\mathcal{G}} &= \boldsymbol{\mathcal{G}}_{\mathrm{p}} \oplus \boldsymbol{\mathcal{G}}_{\mathrm{g}}, \\ \text{where } \ \boldsymbol{\mathcal{V}} = \boldsymbol{\mathcal{V}}_{\mathrm{p}} \cup \boldsymbol{\mathcal{V}}_{\mathrm{g}}, \ \ \boldsymbol{\mathcal{E}} &= \boldsymbol{\mathcal{E}}_{\mathrm{p}} \cup \boldsymbol{\mathcal{E}}_{\mathrm{g}}, \quad \boldsymbol{W} = \boldsymbol{W}_{\mathrm{p}} \oslash \boldsymbol{W}_{\mathrm{g}}. \end{aligned} \tag{5}$$

where $\cup$ denotes the union of two sets, $\oslash$ indicates diagonal concatenation. After hypergraph fusion, a vertex $\boldsymbol{v}_i \in \mathbb{R}^{(2048+69)}$ includes both image features and gene expression, and the number of hyperedges is increased to $k + l$.

This concatenation strategy is designed to bridge the rich morphological insights captured in images with the intricate spatial genetic patterns derived from gene expression data.

Learning global representation of the unified hypergragh. We design the hypergraph convolutional layer as the backbone of MHNN-surv. The hypergraph convolutional layer mainly comprises three steps including node feature transformation, hyperedge feature generation, and node feature aggregation. $\boldsymbol{\mathcal{V}}$ is first multiplied with the learnable parameter θ to obtain the transformed features. Next, the transformed features are gathered by $\boldsymbol{\mathcal{E}}$ to obtain the hyperedge features $\boldsymbol{\mathcal{Y}} = \{\boldsymbol{y}_1, \boldsymbol{y}_2, \ldots, \boldsymbol{y}_m\}$. Finally, the hyperedge features are multiplied to yield the global representation of the WSI by $\boldsymbol{z} = \sum_{i=1}^{m} c_i \boldsymbol{y}_i$, where c_i is the attention score obtained by attention layers.

Survival analysis implementation. The survival analysis model is employed to obtain survival hazard score. It can be categorized into two main types: regression-based approaches and ranking-based approaches. The Cox proportional hazard model is one of the most commonly used regression models in survival analysis. However, it may not effectively distinguish between patients with closely occurring survival times. Thus, we consider a deep ordinal Cox model [17]to generate the hazard score, which adds a ranking-based regularization term to the Cox model. The formulation of the loss function is as follows:

$$\begin{aligned} L = \sum_{i=1}^{P} \delta_i \big(\sigma(\boldsymbol{z}_i) - \log \sum_{j \in R(t_i)} \exp(\sigma(\boldsymbol{z}_j)) \\ + \sum_{j \in R(t_i)} I(i,j) \max(0, 1 - \exp(\sigma(\boldsymbol{z}_i) - \sigma(\boldsymbol{z}_j))) \big), \end{aligned} \tag{6}$$

where P denotes the number of patients, δ_i is the censoring indicator, and $R(t_i)$ represents the set of patients still at risk at time t_i. The function $\sigma(\boldsymbol{z})$ calculates the hazard risk using a multilayer perceptron. The indicator function $I(i, j) = 1$ if patients i and j form a comparable ranking pair, and 0 otherwise.

4 Experiments and Results

4.1 Experimental Settings

Dataset. In this study, the testing dataset is the Breast Invasive Carcinoma (BRCA) dataset extracted from Cancer Genome Atlas (TCGA) [19], with 99

Table 1: Comparison results with SOTA methods in survival prediction (C-Index).

	Model	BRCA		Model	BRCA
WSI only	SCNN [24]	0.558	WSI+ Gene	GSCNN [26]	0.616
	DeepConvSurv [22]	0.544		PAGE-NET [29]	0.608
	Histology CNN [20]	0.571		MCAT [27]	0.617
	DSCA [28]	0.587		Pathomic Fusion [21]	0.625
Gene only	Cox-EN [27]	0.598		GC-SpLem [30]	0.628
	Cox-PASNet [23]	0.605		PMFN-SSL [25]	0.631
	WSI+Spatial Gene			**MHNN-surv**	**0.673**

patient samples. We processed over 1065 gigapixel images from the BRCA case, extracting 41229 patches for detailed analysis. **Evaluation Metrics.** We employed the most popular evaluation metrics in survival analysis, the concordance index (C-index) [20] which estimates the probability of concordance between predicted and observed responses,

$$C = \frac{1}{n} \sum_{i \in \{1 \ldots N | \delta_i = 1\}} \sum_{t_j > t_i} I(p_i > p_j), \tag{7}$$

where n represents the number of comparable pairs, $I[.]$ is the indicator function, t_i (t_j) denotes the actual observed time, and p_i (p_j) is the predicted risk score. The C-index spans the range from 0.5 to 1. The higher C-index represents the more accurate survival prediction.

4.2 Experimental Results

As shown in Table 1, our study highlights the superior performance of the MHNN-surv model in predicting breast cancer survival by integrating spatial gene expression data with pathological imaging. In comparison to state-of-the-art unimodal models, MHNN-surv achieves superior performance. In detail, the traditional gene-based models, such as Cox-EN [27] and CoxPASNet [23], are limited to genetic information, lacking the ability to capture the morphological complexities evident in pathological images. Conversely, models that focus solely on WSI, including SCNN [24], DeepConvSurv [22], Histology CNN [20], and DSCA [28], offer valuable insights into the physical structure of tumors but miss out the genetic context. Furthermore, MHNN-surv maintains its competitively superior performance in comparison of other multimodal fusion models such as GSCNN [26], PAGE-Net [29], MCAT [27], Pathomic Fusion [21], GC-SPLem [30], and PMFN-SSl [25]. The unique aspect of our proposed model is the incorporation of spatially resolved gene expression data, which introduces a spatial context to the genetic information. This achieves a deeper understanding of the tumor environment, enhancing the predictive capabilities of our proposed model and outperforming conventional multimodal approaches.

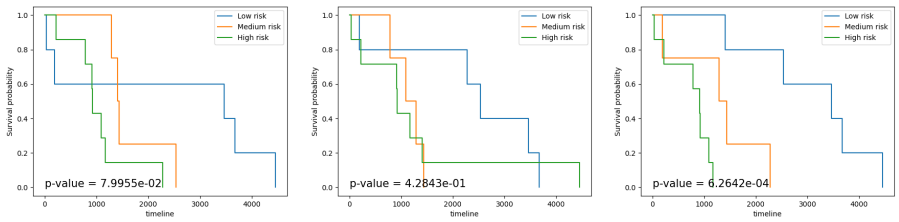

(a) WSI **(b)** Gene **(c)** WSI+Spatial Gene

Fig. 2: The KM-estimation curves of MHNN-surv on TCGA-BRCA.

Table 2: Experimental Results on Ablation Study

Model	MHNN-g	MHNN- ic	MHNN-icc	MHNN-icg	MHNN-surv
BRCA	0.601	0.633	0.651	0.647	0.673

The experiments are also extended to the prognostic differentiation between high and low-risk groups, utilizing univariate KM estimation as depicted, as illustrated in Fig. 2. All samples are grouped via survival risk by MHNN-surv. The reliability of our results is further demonstrated by the significant differences in p-values and probability curves between the groups. In conclusion, the experimental results demonstrate the superiority of the proposed MHNN-surv model in comparison to both unimodal and multimodal models on breast cancer survival prediction, by leveraging spatially resolved gene expression data alongside pathological imaging. Furthermore, MHNN-surv leverages the fusion of hypergraphs on diverse modalities, with comprehensive information for survival analysis, thus achieving accurate prognostic predictions.

4.3 Ablation Experiments for MHNN-surv

To validate the contributions of each module within our methodology, the ablation experiments are performed. These experiments investigate the individual and combined effects of utilizing image coordinates in **MHNN-ic**, augmenting the coordinates with RGB data in **MHNN-icc**, integrating spatial genomic data alongside image coordinates in **MHNN-icg**, and focusing exclusively on spatial genomic data in **MHNN-g**. As reported in Table 2, demonstrate the superior prognostic accuracy of our comprehensive model **MHNN-surv** which integrates all aforementioned modalities, particularly highlighting the importance of spatial genomic data in enhancing cancer suivival predictions.

Meanwhile, the experimental results have also proven that the hypergraph-based fusion technique achieves superior performance compared to the traditional unimodal or multimodal methods on WSI-only, Gene-only, and Multimodal data in table 1, respectively. The main reason is that leveraging the fusion

of hypergraphs from diverse modalities with comprehensive information enables accurate prognostic prediction.

5 Conclusion

In this work, we propose a multimodal hypergraph neural network for breast cancer survival analysis that merges histopathology images with spatial genomics, namely MHNN-surv. It leverages the fusion of hypergraphs on diverse modalities to enhance cancer prognostics performance with spatial gene expression insights. MHNN-surv enriches breast cancer research by offering comprehensive and deep insights into the tumor microenvironment, which may facilitate future research in personalized medicine in breast cancer prognosis and other medical research.

Acknowledgments. This work was supported in part by the Key-Area Research and Development Program of Guangdong Province (2021B0909060002), the China Postdoctoral Science Foundation (2023M730752), the Guangdong Provincial Key Laboratory IRADS (2022B1212010006, R0400001-22), the National Key Research and Development Program of China (2022YFE0112200, 2022YFA1004800), the National Natural Science Foundation of China (U21A20520, 62325204,T2350003,T2341007,12131020, 31930022), and the Key-Area Research and Development Program of Guangzhou City (202206030009).

Disclosure of Interests. The authors have no competing interests to declare that are relevant to the content of this article.

References

1. Nagy,Á., Munkácsy,G. and Győrffy,B. Pancancer survival analysis of cancer hallmark genes. Sci Rep 11, 6047 (2021).
2. Shrivastavat, S.S., Sant, A., Aharwal, R.P.: An overview on data mining approach on breast cancer data. Int. J. Adv. Comput. Res. 3, 256 (2013)
3. Xie, J., Pu, X., He, J. et al: Survival prediction on intrahepatic cholangiocarcinoma with histomorphological analysis on the whole slide images. Comput. Biol. Med. 146, 105520 (2022).
4. He, X., Liu, X., Zuo, F. et al.: Artificial intelligence-based multi-omics analysis fuels cancer precision medicine. Semin. in Cancer. Biol. 88, 187–200 (2023).
5. He, X., Liu, X., Zuo, F. et al.: Artificial intelligence-based multi-omics analysis fuels cancer precision medicine. Semin. in Cancer. Biol. 88, 187–200 (2023).
6. Tong, L., Mitchel, J., Chatlin, K. et al. Deep learning based feature-level integration of multi-omics data for breast cancer patients survival analysis. BMC. Med. Inform. Decis. Mak. 20, 225 (2020).
7. Győrffy, B.: Survival analysis across the entire transcriptome identifies biomarkers with the highest prognostic power in breast cancer. Comput. Struct. Biotech. 19, 4101–4109 (2021).
8. Zhang, H., Cheng, M., Ji, L. et al.: Utilizing tumor microenvironment microbial profiles and host gene expressions for survival subtyping in diverse types of cancers. bioRxiv. 2023.05. 18.541268 (2023).

9. Fu, T., Dai, LJ., Wu, SY. et al. Spatial architecture of the immune microenvironment orchestrates tumor immunity and therapeutic response. J. Hematol. Oncol. 14, 98 (2021)
10. Malagoli Tagliazucchi, G., Wiecek, A.J., Withnell, E. et al. Genomic and microenvironmental heterogeneity shaping epithelial-to-mesenchymal trajectories in cancer. Nat. Commun. 14, 789 (2023).
11. Shi, Zhen-Duo, et al. Tumor cell plasticity in targeted therapy-induced resistance: mechanisms and new strategies. Signal Transduction and Targeted Therapy 8.1 (2023): 113.
12. Di, Donglin, et al. Generating hypergraph-based high-order representations of whole-slide histopathological images for survival prediction. IEEE Trans. Pattern Anal. Mach. Intell. 45.5 (2022): 5800-5815.
13. Feng, Yifan, et al. Hypergraph neural networks. in AAAI, 33.01 (2019): 3558-3565.
14. Karim, M. R., Wicaksono, G., Costa, I. G. et al. Prognostically relevant subtypes and survival prediction for breast cancer based on multimodal genomics data. IEEE Access 7 (2019): 133850-133864.
15. Cheerla, A., and Gevaert, O. Deep learning with multimodal representation for pancancer prognosis prediction. Bioinformatics 35.14 (2019): i446-i454.
16. Palmal, S., Arya, N., Saha, S. et al. Integrative prognostic modeling for breast cancer: Unveiling optimal multimodal combinations using graph convolutional networks and calibrated random forest. Applied. Soft. Computing., 154, 111379 (2024).
17. Lin, D. Y., Wei, L. J., and Ying, Z. Checking the Cox model with cumulative sums of martingale-based residuals. Biometrika 80.3 (1993): 557-572.
18. Bender R, Augustin T, Blettner M. Generating survival times to simulate Cox proportional hazards models. Statistics in medicine. 2005 Jun 15;24(11):1713-23.
19. C. Kandoth, M.D. McLellan, F. Vandin, K. et al. Mutational landscape and significance across 12 major cancer types, Nature 502 (7471) (2013) 333–339.
20. H. Steck, B. Krishnapuram, C. Dehing-Oberije, P. et al. "On ranking in survival analysis: Bounds on the concordance index," Adv. Neural Inf. Process. Syst., vol. 20, 2007.
21. R.J. Chen, M.Y. Lu, J. Wang. et al. Pathomic fusion: an integrated framework for fusing histopathology and genomic features for cancer diagnosis and prognosis, IEEE Trans. Med. Imaging 41 (4) (2020) 757–770.
22. X. Zhu, J. Yao, J. Huang, Deep convolutional neural network for survival analysis with pathological images, in: 2016 IEEE International Conference on Bioinformatics and Biomedicine, BIBM, IEEE, 2016, pp. 544–547.
23. Hao, J., Kim, Y., Mallavarapu, T. et al. Cox-PASNet: pathway-based sparse deep neural network for survival analysis. in BIBM, 2018, pp. 381–386.
24. Mobadersany, P., Yousefi, S., Amgad, M. et al. Predicting cancer outcomes from histology and genomics using convolutional networks, Proc. Natl. Acad. Sci., 115 (13) (2018) E2970–E2979.
25. Li, Le, et al. PMFN-SSL: Self-supervised learning-based progressive multimodal fusion network for cancer diagnosis and prognosis. Knowledge-Based Systems (2024): 111502.
26. Simon, N., Friedman, J., Hastie, T. et al. Regularization paths for Cox's proportional hazards model via coordinate descent, J. Stat. Softw. 39 (5) (2011) 1
27. Steck, H., Krishnapuram, B., Dehing-Oberije, C. et al. On ranking in survival analysis: Bounds on the concordance index. Adv. Neural Inf. Process. Syst., vol. 20, (2007).

28. Liu, P., Fu, B., Ye, F. et al. DSCA: A dual-stream network with crossattention on whole-slide image pyramids for cancer prognosis, Expert Syst. Appl. 227 (2023) 120280.
29. Hao, J., Kosaraju, S. C., Tsaku, N. Z. et al. PAGE-Net: interpretable and integrative deep learning for survival analysis using histopathological images and genomic data, in: Pacific Symposium on Biocomputing 2020, World Scientific, 2019, pp. 355–366.
30. Xie, Y., Niu, G., Da, Q. et al. Survival prediction for gastric cancer via multimodal learning of whole slide images and gene expression, in BIBM, 2022, pp. 1311–1316.